Collective modes and electronic Raman scattering in the cuprates

F. Venturini, Umberto Michelucci, T. P. Devereaux, Arno P. Kampf

Collective Modes and Electronic Raman Scattering in the Cuprates

F. Venturini[1], U. Michelucci[2], T.P. Devereaux[3], and A.P. Kampf[2]

[1]Walther-Meissner-Institut, Walther-Meissner-Str. 8, 85748 Garching, Germany
[2]Theoretische Physik III, Universität Augsburg, 86135 Augsburg, Germany
[3]Department of Physics, University of Waterloo, Waterloo, Canada, N2L 3G1

While the low frequency electronic Raman response in the superconducting state of the cuprates can be largely understood in terms of a d-wave energy gap, a long standing problem has been an explanation for the spectra observed in A_{1g} polarization orientations. We present calculations which suggest that the peak position of the observed A_{1g} spectra is due to a collective spin fluctuation mode.

1. INTRODUCTION

In spite of the considerable efforts to explain the experimental Raman spectra of cuprate superconductors, the A_{1g} superconducting response is not yet completely understood. It has been shown that the theoretical description of the A_{1g} Raman response was very sensitive to small changes in the Raman vertex harmonic representations, yielding peak positions varying between Δ and 2Δ [1]. However, the data show peaks consistently slightly above Δ for both YBCO and BSCCO.

In this paper we present calculations suggesting that the A_{1g} peak position is largely controlled by a collective spin fluctuation (SF) mode near 41 meV, consistent with inelastic neutron scattering (INS) observations [2,3]. We show that the A_{1g} response is strongly modified by the SF term and is not sensitive to small changes in the Raman vertex. The experimental peak position is well reproduced by our model whereas the B_{1g} and B_{2g} response remain essentially unaffected by the SF mode.

2. MODEL CALCULATION

The CuO_2 bilayer is modeled by a tight binding band structure with a nearest (t) and a next nearest neighbor hopping (t') parameter and an inter-plane hopping given by [4]

$$t_\perp(\mathbf{k}) = 2t_\perp \cos(k_z)[\cos(k_x) - \cos(k_y)]^2. \qquad (1)$$

k_z can be 0 or π, for bonding or anti-bonding bands of the bilayer, respectively.

The spin susceptibility (χ_s) is modeled by extending the weak coupling form of a $d_{x^2-y^2}$ superconductor to include antiferromagnetic spin fluctuations by an RPA form with an effective interaction $\bar{U}$; i.e. $\chi_s = \chi_0/(1 - \bar{U}\chi_0)$ where χ_0 is the simple bubble in the d-wave state. This form of the spin susceptibility is motivated by the fact that it contains a strong magnetic resonance peak at $\mathbf{q} = \mathbf{Q} = (\pi, \pi, \pi)$ which was proposed [4] to explain the INS resonance at energies near 41 meV in YBCO [2] and BSCCO [3].

The Raman response function in the superconducting state is evaluated using Nambu Green's functions. The spin fluctuations contribute to the Raman response via a 2-magnon process as shown in Fig. 1 [5] where a schematic representation of the Feynman diagrams of the SF and the bubble contribution is plotted. For the electronic propagators we have used the bare BCS Green's functions and a d-wave superconducting gap $\Delta_\mathbf{k} = \Delta_0[\cos(k_x) - \cos(k_y)]/2$.

The total Raman response is calculated in the gauge invariant form which results from taking into account the long wavelength fluctuations of the order parameter [1]. The total Raman susceptibility is thus given by

$$\chi_{tot}(\mathbf{q} = \mathbf{0}, i\Omega) = \chi_{\gamma\gamma}(\mathbf{0}, i\Omega) - \frac{\chi_{\gamma 1}^2(\mathbf{0}, i\Omega)}{\chi_{11}(\mathbf{0}, i\Omega)} \qquad (2)$$

where $\chi_{ab}(\mathbf{q} = \mathbf{0}, i\Omega)$ is determined according to Fig. 1. The analytical continuation to the real axis is performed using Padé approximants.

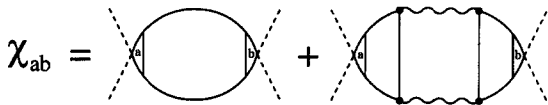$$\chi_{ab} = \text{(diagram)} + \text{(diagram)}$$

Figure 1. Feynman diagram considered for the particle-hole and SF contributions. Dashed, wiggly and solid lines represent photon, SF and electronic propagators, respectively. The solid circle marks the coupling $\bar{U}$ for the electron-SF vertex.
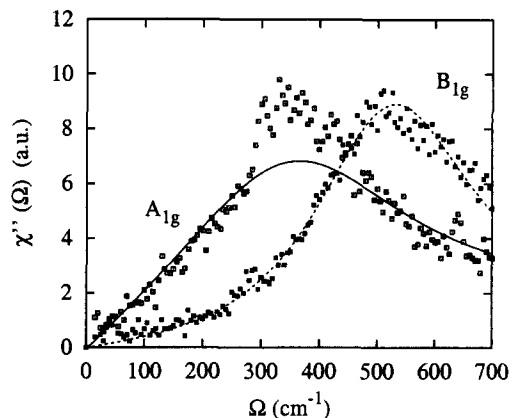

Figure 2. Comparison of the A_{1g} and B_{1g} total response with Bi-2212 data taken from Ref. [6]. The values of the parameters are $\Delta_0/t = 0.25$, $t'/t = 0.45$, $t_\perp/t = 0.1$, $\langle n \rangle = 0.85$, $\bar{U}/t = 1.3$, $t = 130$ meV.

We have used several different forms for the Raman vertex γ which possess the correct transformation properties required by symmetry. Our calculations show that the SF term yields vanishingly small corrections to the response in the B_{1g} and B_{2g} channels, but contributes substantially to the A_{1g} channel. The shape of the total response in the A_{1g} geometry is mainly dependent on the value of the effective interaction $\bar{U}$. Variations of $\bar{U}$ change the relative magnitude of the two diagrams summed in Fig. 1, changing the position of the peak in A_{1g} geometry. Importantly, we find that the A_{1g} response shows little dependence on the form used for the vertex: $\cos(kx) + \cos(ky)$, $\cos(kx)\cos(ky)$, or the vertex calculated in an effective mass approximation. These results can be explained by symmetry reasons given that the SF propagator is strongly peaked for $\mathbf{Q}$ momentum transfers.

3. COMPARISON WITH DATA

We compare the calculated Raman response with the experimental spectra of an optimally doped Bi-2212 sample [6] in Fig. 2. Adding the SF contribution leads to a shift of the peak position from near $\sim \Delta_0$ for $\bar{U} = 0$ to higher frequencies, allowing a better agreement with the experimental relative positions of the peaks in A_{1g} and B_{1g} geometries. For the fit we have adjusted t to achieve a good agreement with the B_{1g} channel, obtaining $t = 130$ meV, and then adjusted $\bar{U}$ to match both the A_{1g} peak position as well as the peak in the SF propagator to be consistent with the INS peak at 41 meV.

From this work we conclude that including the SF contribution in the Raman response solves the previously unexplained sensitivity of the A_{1g} response to small changes in the Raman vertex. Whereas the SF (two-magnon) contribution controls the A_{1g} peak, the B_{1g} and B_{2g} scattering geometries are essentially unaffected and determined by the bare bubble alone.

REFERENCES

1. T.P. Devereaux et al., Phys. Rev. B **51**, 16336 (1995); ibid. **54**, 12523 (1996).
2. H.F. Fong et al., Phys. Rev. Lett. **75**, 316 (1995); Nature **398**, 588 (1999).
3. H.A. Mook et al., Phys. Rev. Lett. **70**, 3490 (1993).
4. N. Bulut et al., Phys. Rev. B **53**, 5149 (1996).
5. A.P. Kampf and W. Brenig, Z. Phys. B- Condensed Matter **89**, 313 (1992).
6. T.P. Devereaux et al., Phys. Rev. Lett. **72**, 3291 (1994).